

# Improvement of the power conversion efficiency of a personal computer

ISSN 1755-4535

Received on 3rd April 2015

Revised on 18th January 2016

Accepted on 18th February 2016

doi: 10.1049/iet-pel.2015.0234

www.ietdl.org

Te Huang<sup>1</sup> ✉, Ying-Wen Bai<sup>2</sup>, Hung-Ming Kuan<sup>2</sup>

<sup>1</sup>Graduate Institute of Applied Science and Engineering, Fu Jen Catholic University, No. 510, Zhongzheng Road, Xinzhuang District, New Taipei City 24205, Taiwan

<sup>2</sup>Department of Electrical Engineering, Fu Jen Catholic University, No. 510, Zhongzheng Road, Xinzhuang District, New Taipei City 24205, Taiwan

✉ E-mail: 497598030@mail.fju.edu.tw

**Abstract:** Most low-power PC design research focuses on the power consumption of devices in the system, in order to reduce the consumption of the peripheral components while the system is in the idle state. In this design, the power conversion efficiency of the multi-phase pulse width modulation power regulator can be improved by using the auto-phase switching control scheme. The external load-sensing circuit is used to both monitor the output current and to change the regulator to a different operation method automatically. This design is dependent on the different loading to set the optimised operation phase. The power conversion efficiency can be maintained from 88.19 to 93.41%, when the load current is changed from 1.06 to 119 A.

## 1 Introduction

According to Moore's law, the number of transistors in an integrated circuit (IC) doubles every 18 months. This means that the power consumption will increase because of more transistors. This design is a simple way to obtain a better performance from the central processing unit (CPU), which improves the operating frequency of the CPU. However, a faster CPU operating frequency produces more switching loss by the transistors in the CPU. Some other ways to better the CPU's performance are either by increasing the parallel operational capability of the CPU, by increasing the pipeline, or by performing hyper threading. These performance enhancements increase the number of the transistors in the CPU, thereby increasing the power consumption. At present, the CPU power consumption limit of a PC is 150 W.

This paper is a modification and improvement of the previous auto phase switching pulse width modulation (PWM) design [1], and use hysteresis both to avoid the phase frequency switching and to increase the operating system efficiency.

The PWM DC–DC buck voltage regulator is often used not only in digital home appliances but also in PCs [2, 3]. The PWM power regulator is the most efficient and applicative regulator in use today. It is used in PCs, home appliances, and communication equipment because of its high stability and power conversion efficiency. The PWM power regulators are combined with a PWM controller, a MOSFET driver, and MOSFETs. Generally the output current of a single-phase PWM power regulator is about 20–30 A, due to its traditional MOSFET structure, its semiconductor process, its volume, its cost, and other factors. To provide the large amount of current needed for the CPU, the multi-phase PWM power regulator is commonly used [4, 5].

To improve the power conversion efficiency of the PWM power regulators, there has been much research which has focused both on the circuit design and on modifying the architecture [6, 7]. Two other ways that can be used to improve the efficiency are by using either the zero voltage switching (ZVS) or the zero current switching (ZCS) methods. These two methods focus on the effective circuit modification currently used both to improve the ZCS and ZVS and also to reduce switching loss [8–10].

To provide more power for the CPU, the number of phases of the PWM power regulator has to be increased [11, 12]. When the system

is in the idle state, the new power control technique reduces the power consumption of the CPU. Consequently, in the idle state the CPU both reduces its operating frequency and shuts down both its unused cores and circuits [13]. Furthermore, the system is in the light operation mode while the user is either surfing the Internet, watching movies, or processing documents. The disadvantage of the multi-phase PWM power regulator is its poor efficiency while in the light operation mode [14].

Fig. 1 shows six power conversion efficiency curves from the single-phase to the six-phase PWM power regulator, respectively. The single-phase PWM power regulator as shown by the 'plus' mark is of higher efficiency with light loads, but this efficiency rapidly declines as the load current is increased. In contrast, the six-phase PWM power regulator as shown by the 'X' mark has a higher efficiency at heavy loads, but this efficiency becomes lower than that of the single-phase at light loads. Thus, some research is currently being conducted with respect to the light load efficiency improvement of the multi-phase PWM power regulators [15–17].

Table 1 compares the efficiency of the single-phase and the six-phase PWM power regulator while the load currents are 10 and 40 A. The single-phase PWM power regulator obtains higher conversion efficiency with a reduced load current. However, the six-phase has higher conversion efficiency when used with a greater load current.

Section 2 explains the design and implementation of the multi-phase auto-control method. Section 3 shows the measurement result. The final section summarises the conclusion and provides a look at future possibilities.

## 2 Multi-phase auto-control method

On the basis of the power conversion efficiency curves shown in Fig. 1, it is proposed to use the auto-phase control method to control the multi-phase PWM power regulator [18–21]. The number of phases for the multi-phase PWM power regulator changes depends on the output current. The PWM operating phases reduce under a light load condition and increase under a heavy load, thus obtaining the highest possible power conversion efficiency from a light load to a heavy load.

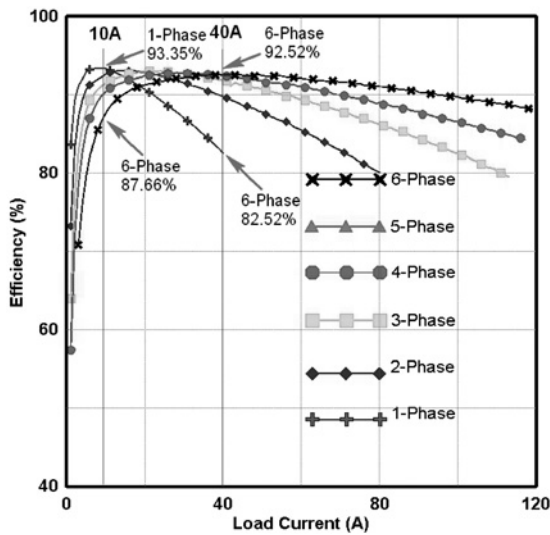


Fig. 1 Multi-phase PWM power conversion efficiency

There are three parts of the multi-phase auto-control design. The first is the output current detection, the second is the setting up of both the comparator and the switching point, and the third is the multi-phase control circuit. The block diagram is shown in Fig. 2.

### 2.1 Output current detection

A high precision resistor is added at the load side in order to obtain the output current ( $I_{OUT}$ ) by using the differential voltage of the operational-amplifier (OP-Amp.), as shown in Fig. 3.

By using the circuit design in Fig. 3, the output current can be detected through the output voltage conversion of the OP-Amp. Equation (1) shows the current-to-voltage conversion. The output current through  $R_{SHUNT}$  is  $I_{OUT}$ . The calculated output voltage of OP-Amp. ( $V_{IMON}$ ) can be defined as

$$\begin{aligned}
 V_{IMON} &= I_{OUT} \times R_{SHUNT} \times \left( \frac{R3}{R3 + R1} \right) \times \left( 1 + \frac{R4}{R2} \right) \\
 &\Rightarrow I_{OUT} \times 0.001 \times \left( \frac{143 \text{ k}}{143 \text{ k} + 2.23 \text{ k}} \right) \times \left( 1 + \frac{143 \text{ k}}{2.32 \text{ k}} \right) \\
 &= I_{OUT} \times 0.0616
 \end{aligned} \tag{1}$$

The dot line of Fig. 6a is a graph of (1). The horizontal axis is the output current  $I_{OUT}$  whose output ranges from 0 to 120 A. The vertical axis is the output current conversion result of the voltage  $V_{IMON}$  whose range is between 0 and 7.392 V. By utilising this diagram and (1), the output current can be calculated from the  $V_{IMON}$ .

### 2.2 Setting up comparator and switching points

There are five reference voltages ( $V_{REF}$ ) defined for the switching points as shown in Table 2. This method is used to compare  $V_{REF}$  with the  $V_{IMON}$  to switch to different operating phases.

Table 1 Power conversion efficiency of a single-phase and a six-phase PWM power regulator

Operation phases	10 A	40 A
single-phase, %	93.35	82.52
six-phase, %	87.66	92.52

When the  $V_{IMON}$  is higher than 0.7 V ( $V_{REF}$ ), the corresponding output current is 11.36 A, and the multi-phase PWM power regulator is switched to the two-phase mode. When the  $V_{IMON}$  reaches 1.6 V, the output current is equal to 25.96 A, and the regulator is switched to the three-phase mode. If the  $V_{IMON}$  is >2.1 V, the output current is >34.08 A, and the regulator is then switched to the four-phase mode. If the  $V_{IMON}$  is >2.8 V, the output current is >45.44 A, and the regulator is automatically switched to the five-phase mode. If the  $V_{IMON}$  is >4.2 V, the output current is >68.14 A, and the regulator is instantly switched to the six-phase mode.

### 2.3 Hysteresis circuit

The hysteresis circuit is used in the PWM-phase control to avoid frequent phase switching. The  $R6$  is used for the OP-Amp. hysteresis. The hysteresis OP-Amp. circuit is shown in Fig. 4a.

The hysteresis is used in the PWM on-off control to avoid overly frequent turning on and off of the PWM. In the simple application, the OP-Amp. controlling the PWM off depends on whether the  $V_{IMON}$  falls below or above the reference voltage  $V_{REF}$ . With hysteresis, the OP-Amp. remains on until the  $V_{IMON}$  rises somewhat above the set point  $V_{REF}$ , and then remains off until the  $V_{IMON}$  falls to a value below the set point. The switching levels are the high- and low-threshold voltages of the  $V_{TH}$  and the  $V_{TL}$ , respectively. The  $V_{REF}$  is set as the  $V_{TH}$ , the  $V_{IMON}$  as the  $V_{IN}$ , and the PWM control is set as the  $V_{OUT}$  in the OP-Amp. control circuit. When the  $V_{IN}$  increases and either reaches or is greater than the  $V_{TH}$ , which means that load current is increasing, the output voltage  $V_{OUT}$  is +12 V in order to turn the PWM phase on. When the load current decreases, the  $V_{OUT}$  remains at +12 V. As the load current continues to decrease and reaches the  $V_{TL}$ , the  $V_{OUT}$  becomes ~0 V. The hysteresis design thus can avoid any frequent phase of turning on and off, as shown in Fig. 4b.

When the  $V_{IMON}$  is lower than 3.89 V ( $V_{REF}$ ), the corresponding output current is 63.13 A, and the multi-phase PWM power regulator is switched to the five-phase mode. When the  $V_{IMON}$  reaches 2.65 V, the output current is equal to 43 A, and the regulator is switched to the four-phase mode. If the  $V_{IMON}$  is <1.99 V, the output current is <32.3 A. The regulator then switches to the three-phase mode. If the  $V_{IMON}$  is <1.51 V, the output current is <24.51 A, and the regulator switches to the two-phase mode. If the  $V_{IMON}$  is <0.66 V, the output current is <10.71 A, and the regulator switches to the single-phase mode.

Fig. 5 is the phase switching circuit which connects the  $V_{IMON}$  to the output current detection circuit to get the corresponding output current. When the  $V_{IMON}$  is less than the  $V_{REF}$ , the output of the  $PWMx\_EN$  logic becomes 0. The switching circuit disconnects the  $PWMx$  to the  $PWMx\_DRV$  and sets the  $PWMx\_OFF$  to logic 1 to disable the PWM of the designated phase. When the  $V_{IMON}$  is higher than the  $V_{REF}$ , the output of the  $PWMx\_EN$  logic becomes 1, and the output connects the  $PWMx$  to the  $PWMx\_DRV$ . The MOSFETs are controlled by the MOSFET driver and in the meantime set the  $PWMx\_OFF$  floating in an acceptable order to enable the PWM of the designated phase. The other phase control methods are the same control methods as in Table 3.

Fig. 6a shows both the  $I_{OUT}$  conversion from the  $V_{IMON}$  and the actual switching point of the multi-phase PWM regulator. The dot line is the designed curve as shown as Fig. 6a; and the black line shows the phase step up while the load increases. When the  $I_{OUT}$  is <11.36 A and the  $V_{IMON}$  is <0.7 V, the PWM regulator will operate in the single-phase mode. When the  $I_{OUT}$  is in the range from 11.36 to 25.96 A, which means that the  $V_{IMON}$  is in the range from 0.7 to 1.6 V, the PWM regulator will operate in the two-phase mode. When the  $I_{OUT}$  reaches 25.96 A and is <34.08 A, this means that the  $V_{IMON}$  reaches 1.6 V, which is <2.1 V, and the PWM regulator will operate in the three-phase mode. When the  $I_{OUT}$  is in the range of 34.08–45.44 A and the  $V_{IMON}$  is in the range of 2.1–2.8 V, the PWM regulator will operate in the three-phase mode. When the  $I_{OUT}$  is 45.44–68.16 A and the  $V_{IMON}$  is 2.8–4.2 V, the PWM regulator will operate in the five-phase

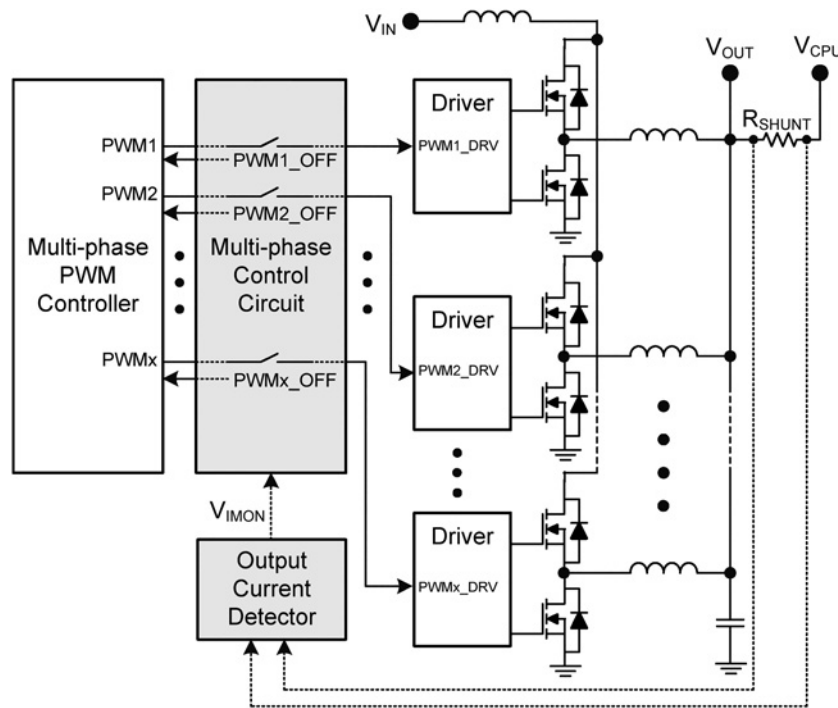


Fig. 2 Block diagram of the multi-phase auto-control method

mode. When the  $I_{OUT}$  reaches 68.16 A and the  $V_{IMON}$  reaches 4.2 V, the PWM regulator will operate in the six-phase mode.

When the  $I_{OUT}$  is decreased, the measured  $V_{IMON}$  is reduced. The operation phases then step down as shown by the grey line, because of the hysteresis.

The measured output current  $I_{OUT}$  and the  $V_{IMON}$  may be viewed in Fig. 6b. The solid line shows the measurement results, and the dotted line shows the simulation results. This result is similar to that of the calculation result.

According to Fig. 6b, by comparing both the measurement and simulation results, if the system has no load, there already is a 0.2984 V  $V_{IMON}$  present. Thus, the  $V_{IMON}$  ranges from 0.2984 V when the  $I_{OUT}$  is initially zero. The power consumption increases and will react in the  $V_{IMON}$ . When the  $I_{OUT}$  increases, the  $V_{IMON}$  is actually similar in proportion to the linear increase.

### 3 Experiment and measurement results

#### 3.1 Methods for measurement of power conversion efficiency

Fig. 7a shows the methods for the measurement of power conversion efficiency. The power source of the PWM regulator is the CPU\_12 V

from the power supply unit. The CPU\_12 V first connects to a multi-meter to observe the input voltage ( $V_{IN}$ ) and then to the PWM regulator input connector. The clamp meter can measure the input current ( $I_{IN}$ ). On the output side, the electronic current load has been set as the output current ( $I_{OUT}$ ) and the second multimeter can observe the output voltage ( $V_{OUT}$ ). An oscilloscope can monitor the output current waveform and the relationship with the control signals, as shown in Fig. 7a. Fig. 7b shows the actual measurement environment of Fig. 7a.

On the basis of the measurement result, the power conversion efficiency ( $\eta$ ) is as shown as

$$\eta = \frac{P_{OUT}}{P_{IN}} = \frac{V_{OUT} \times I_{OUT}}{V_{IN} \times I_{IN}} \quad (2)$$

#### 3.2 Output current and control signals

The change between a light and a heavy load can be observed by the test softwares Prime95 and PiLoop. The first waveform is the current sensing voltage  $V_{IMON}$ , which is a converted voltage signal of the load current, as shown in Fig. 3. The other three waveforms are the enable signals of PWM2–PWM4. They are output signals of

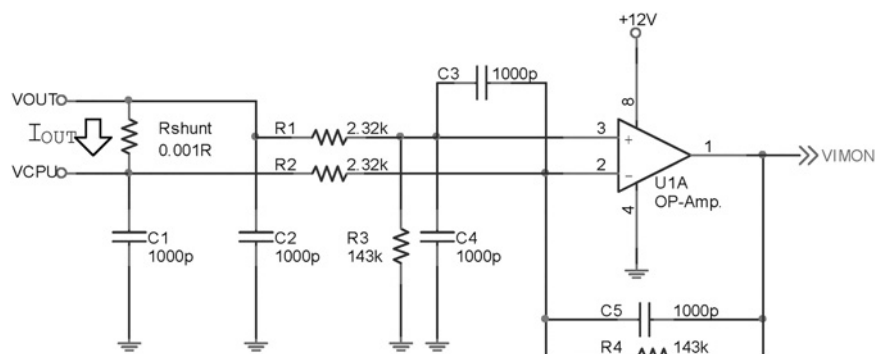
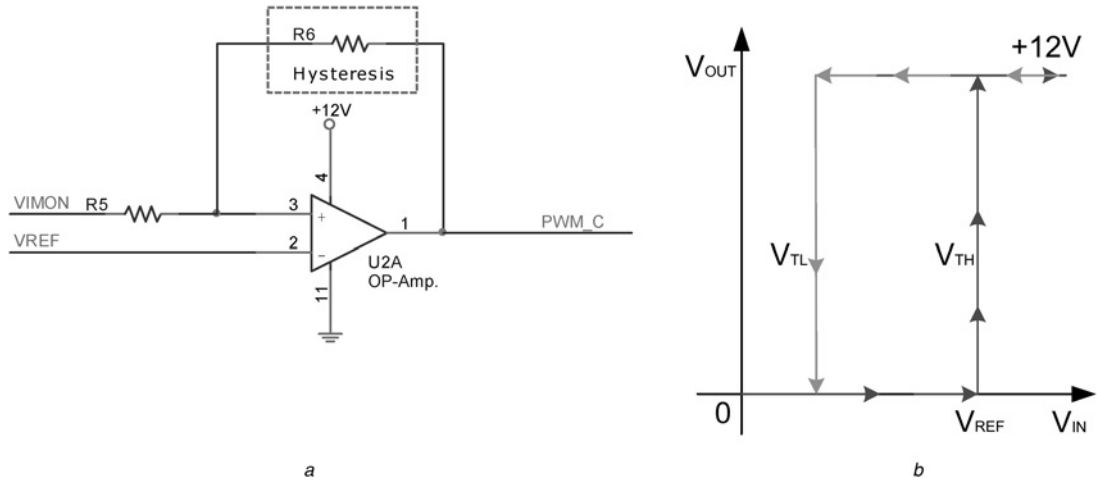


Fig. 3 Output current detection circuit

**Table 2** Switch condition of load current and  $V_{IMON}$

Switch condition	0.7 V	1.6 V	2.1 V	$V_{IMON} > V_{REF}$	2.8 V	4.2 V
load current, A phase	11.36 two-phase	25.96 three-phase	34.08 four-phase		45.44 five-phase	68.14 six-phase



**Fig. 4** Hysteresis design

a Hysteresis OP-Amp. circuit  
b Hysteresis operation method

three specified OP-Amps, which are used to control whether the PWM2–PWM4 is to be turned on or off. The  $V_{IMON}$  is gradually increased by the output current. When the  $V_{IMON}$  reaches 0.7 V, the PWM2\_EN is logic 1, and the PWM controller enables the second phase of the PWM. When the  $V_{IMON}$  reaches 1.6 V, the PWM\_EN3 is triggered and enables the third phase of the PWM. When the  $V_{IMON}$  reaches about 2.1 V, the PWM4\_EN is triggered and enables the fourth phase of the PWM, as shown in Fig. 8a.

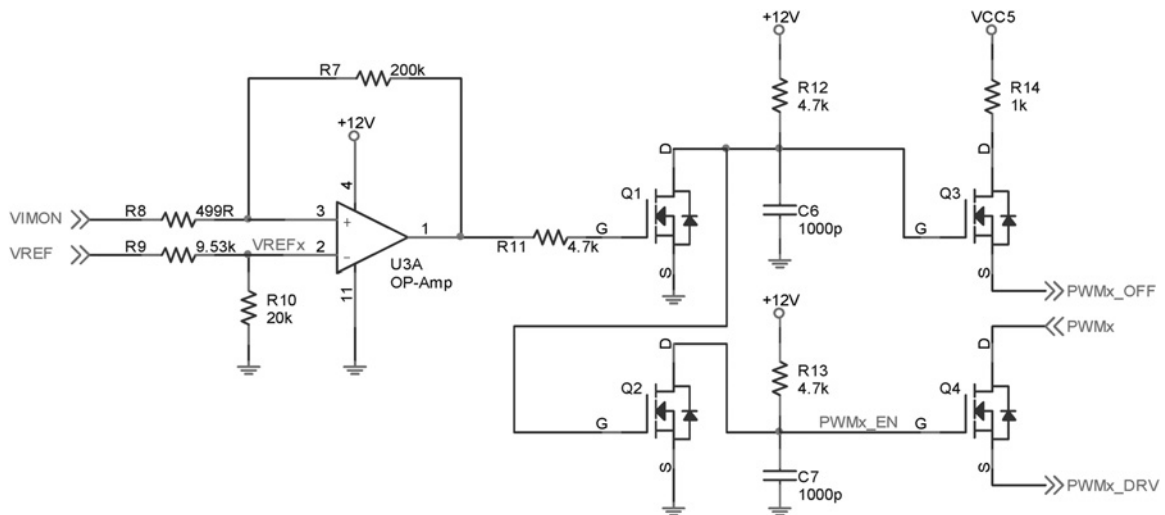
The following waveforms are the  $V_{IMON}$ , and enable the signals of PWM4–PWM6. When the  $V_{IMON}$  reaches at 2.8 V, the PWM5\_EN is triggered and enables the fifth phase of the PWM. When  $V_{IMON}$  arrives at 4.2 V, the PWM6\_EN is triggered and enables the sixth phase of the PWM, as shown in Fig. 8b.

Fig. 8c is the measurement result of the hysteresis control. When the  $V_{IMON}$  triggers the set point  $V_{REF}$ , the PWM2\_EN goes to a high

to turn on the second phase immediately; when the  $V_{IMON}$  decreases, the PWM2\_EN remains in a high until the  $V_{IMON}$  is lower than the low-threshold voltage  $V_{TL}$ . Thus, the hysteresis control helps prevent the PWM2\_EN from turning on and off frequently.

### 3.3 Response time measurement

The first waveform is the reference voltage  $V_{REF}$ , the second waveform is the current sensing voltage  $V_{IMON}$ , the third waveform is the enable signal PWM3\_EN, and the last waveform is the PWM3 signal. When the loading is increased, the result is that the  $V_{IMON}$  is gradually increased. When the  $V_{IMON}$  reaches the  $V_{REF}$  1.6 V, the PWM\_EN3 is asserted and enables the third phase of the PWM. The PWM3 starts to operate immediately, as shown



**Fig. 5** Multi-phase control circuit with hysteresis

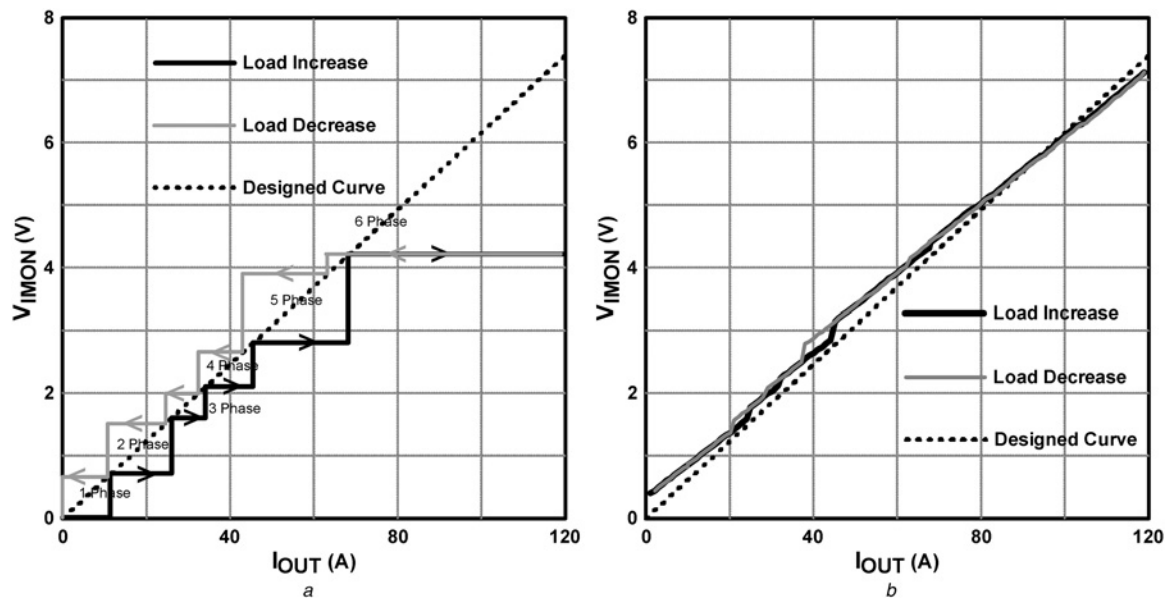


**Fig. 6** Current to voltage conversion curve of the OP-Amp

*a* Multi-phase switching point

*b* Comparison of measurement and calculation results

**Table 3** Switched off condition of the load current and  $V_{IMON}$

Switch condition	3.89 V	2.65 V	1.99 V	$V_{IMON} < V_{REF}$	1.51 V	0.66 V
load current, A	63.13	43	32.3		24.51	10.71
phase	five-phase	four-phase	three-phase		two-phase	single-phase

in Fig. 9*a*. Fig. 9*b* is the detailed waveform of Fig. 9*a*. The response time of the PWM3 enabling is about 30.9  $\mu$ s.

When the loading is decreased, the  $V_{IMON}$  decreases and reaches 1.6 V  $V_{REF}$ . The PWM3 is turned off by means of the hysteresis control; the response time is  $\sim$ 23.5 ms.

### 3.4 Power conversion efficiency measurement

The same devices have been used to measure the power conversion efficiency, including the power supply unit, the CPU, the memory, a

hard disk drive, a keyboard, a mouse, and an operating system (OS). Both the original fixed six-phase mode and the auto-phase switch mode are used for the power efficiency measurement system. Table 4 shows the comparison of both the fixed six-phase system and of this design.

The first test item is idle. The  $I_{IN}$  is 0.532 A and its efficiency is 76.81% for the fixed six-phase system, and the  $I_{IN}$  is 0.444 A and its efficiency is 90.05% for this design. Test item 2 is the MP3 music playback. The  $I_{IN}$  is 0.809 A and the efficiency is 84.13% for the fixed six-phase system; however, the  $I_{IN}$  is 0.734 A and the efficiency

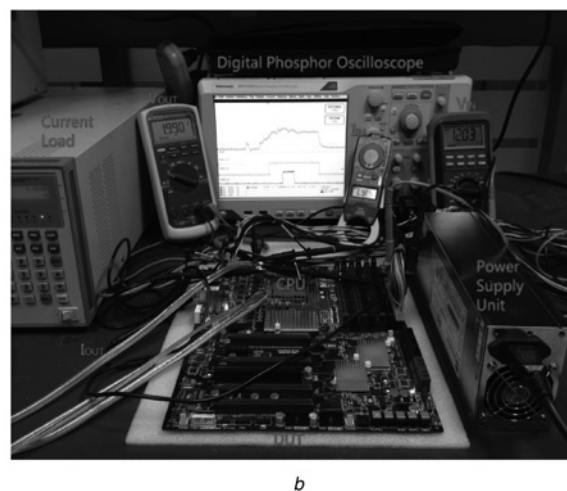
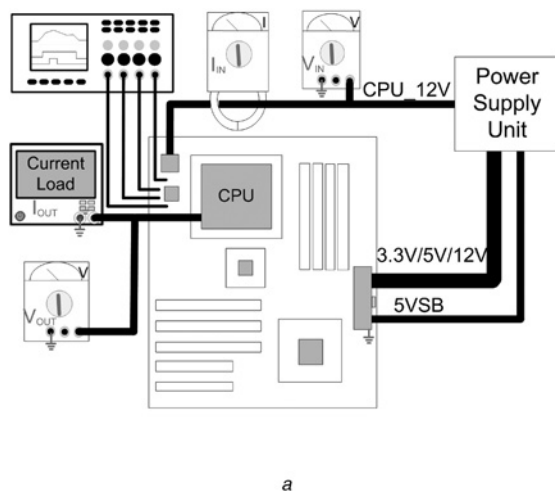
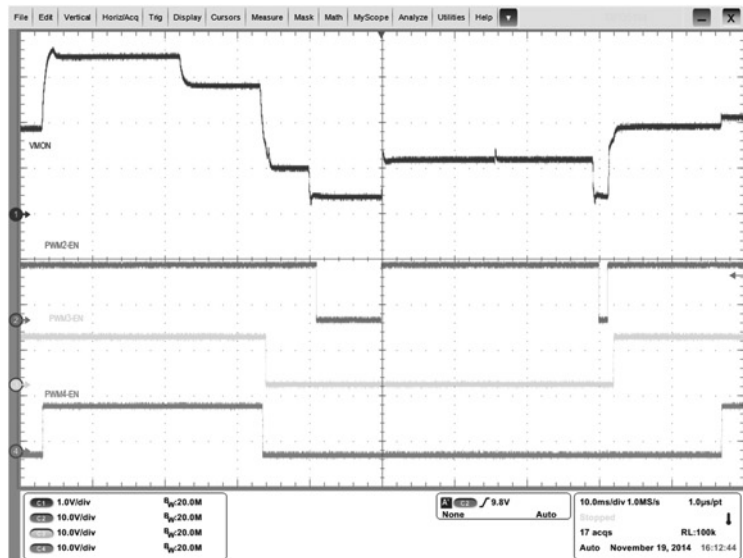


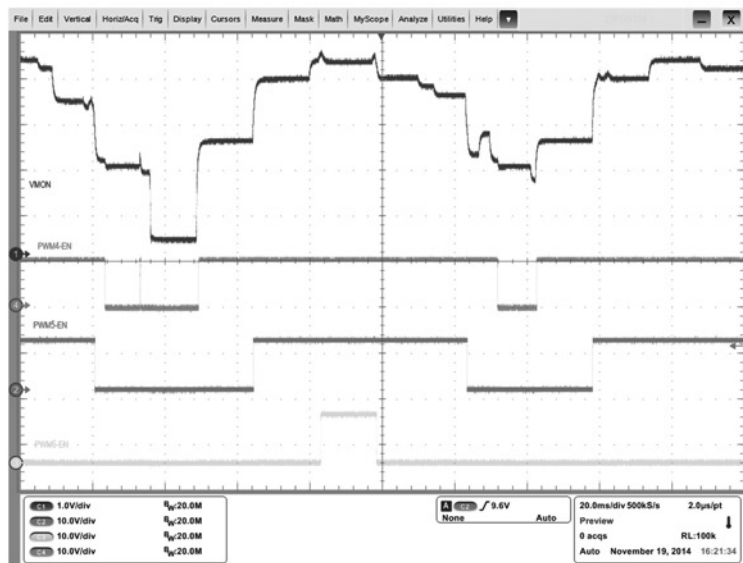
**Fig. 7** Measuring the power conversion efficiency of the PWM regulator

*a* Architecture of the methods used for measurement

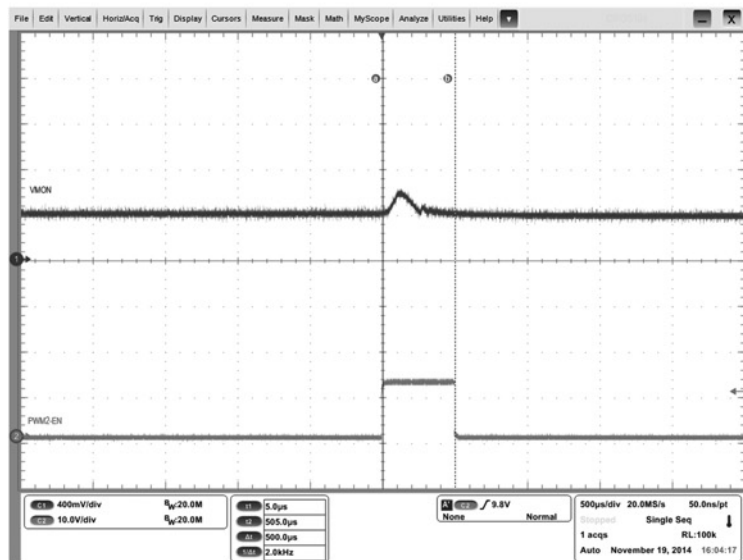
*b* Photograph of the measurement



a



b



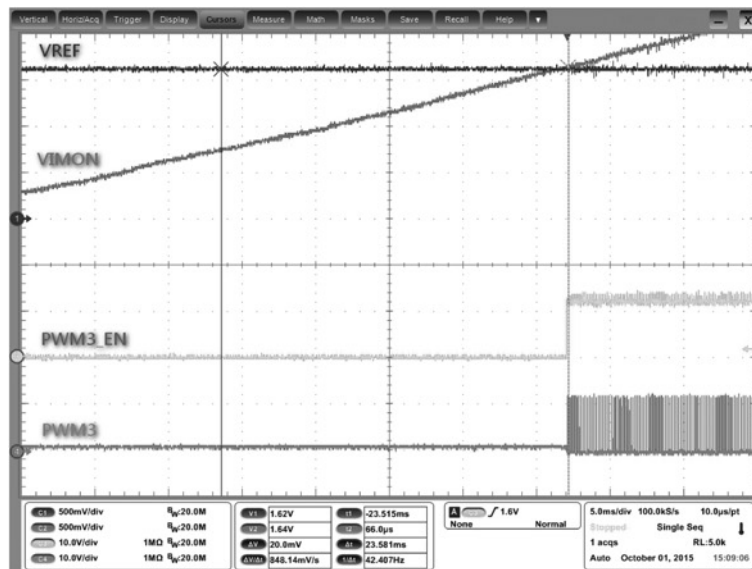
c

**Fig. 8** Control signals of the output current measurement

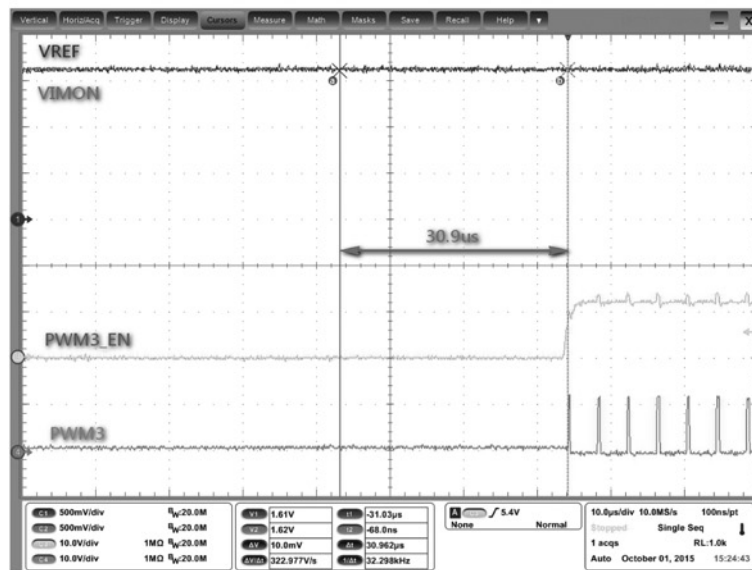
a Control signals of PWM\_EN 2–4

b Control signals of PWM\_EN 4–6

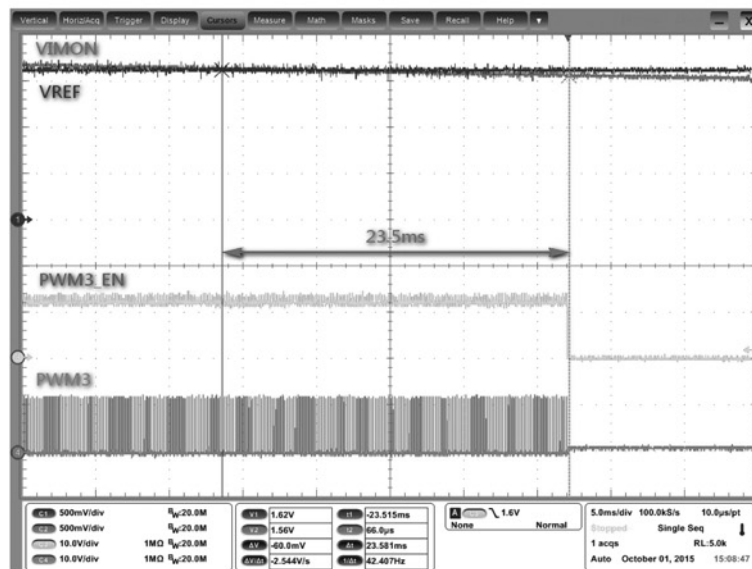
c Hysteresis control measurement of PWM2\_EN



a



b



c

**Fig. 9** Response time measurement

a Response time of PWM3 enabling

b Detail response time of PWM3 enabling

c Response time of PWM3 disabling with hysteresis control

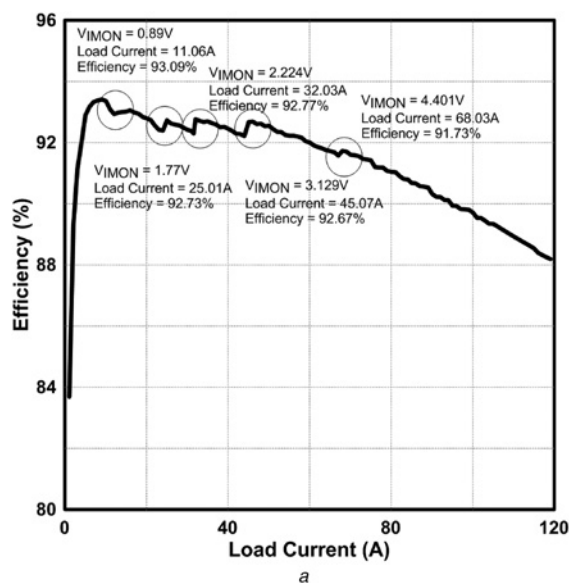
**Table 4** Efficiency comparison table

Control method	Idle, %	Music playback, %	Copy file, %	Video playback, %
fixed six-phase auto control	76.81 90.05	84.13 91.64	84.98 91.54	90.22 92.85

**Fig. 10** Power conversion efficiency measurement

is 91.64% for this design. Test item 3 is file copying; the system copied 100 GB of files for this test. The original design has 0.849 A  $I_{IN}$  and an 84.98% efficiency; however, this design is 0.713 A  $I_{IN}$  and has a 91.54% efficiency. The last test item is movie playback; the system plays a 1080 p high definition video. The original design consists of 1.594 A  $I_{IN}$  and of 90.22% efficiency; however, this design has 1.134 A  $I_{IN}$  and a 92.85% efficiency.

Fig. 10 shows the photo of the power conversion efficiency measurement. The measurement results show the power conversion efficiency which has been improved to 96.85% from the original 76.813 during the typical daily usages. As a result of this design, the power conversion efficiency enhancement ranges from about 2.64 to 13.24%.

**Fig. 11** Measurement results of the power conversion efficiency

a Switch point and power conversion efficiency

b Efficiency comparison of legacy and auto-phase designs

### 3.5 Power conversion efficiency

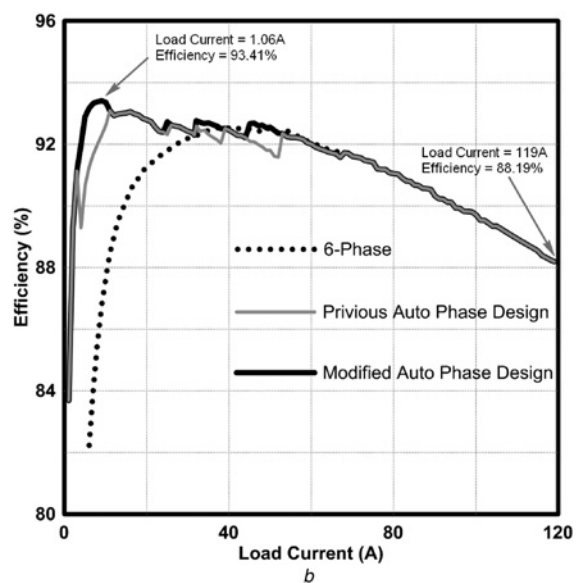
The power conversion loss is reduced by use of the multi-phase auto-control method. The power conversion efficiency is calculated by measuring the results of both the input and the output power consumption.

Fig. 11a is the measurement result of the power conversion efficiency. When the load current is 11.06 A, the  $V_{IMON}$  is 0.89 V, the efficiency is 93.09%, and the system automatically switches to the two-phase operation mode. When the load current is 25.01 A, the  $V_{IMON}$  is 1.77 V, the efficiency is 92.73%, and the system automatically switches to the three-phase mode. When the load current is 32.03 A, the  $V_{IMON}$  is 2.224 V, the efficiency is 92.77%, and the system automatically switches to the four-phase mode. When the load current is 45.07 A, the  $V_{IMON}$  is 3.129 V, the efficiency is 92.67%, and the system automatically switches to the five-phase mode. When the load current is 68.03 A, the  $V_{IMON}$  is 4.401 V, the efficiency is 91.73%, and the system automatically switches to the six-phase mode.

Fig. 11b compares the efficiency both of the legacy six-phase DC–DC PWM regulator and of the previous and modified auto-phase controlled design. The legacy six-phase is shown as a dotted line; the previous auto-phase switching design is shown as a grey line; and the modified auto-phase switching design is shown as a black line. The power conversion efficiency is 93.41% while the output current is 1.06 A. Compared with the legacy fixed six phases DC–DC buck regulator, the power conversion efficiency is approximately a 23% improvement. The power conversion efficiency drops to 88.19% while the output current is 119 A. The system detects the load current and switches to the different phases, so the power conversion efficiency can be maintained at a high level.

## 4 Conclusion

In this paper, the power conversion efficiency can be improved by the multi-phase auto-control method. The OP-Amp. comparator detects the output current and controls the phases of the multi-phase PWM power regulator. The multi-phase auto-control method improves the efficiency of the regulator. This design not only determines the optimum number of phases but also switches phases automatically, thus obtaining a higher degree of power conversion efficiency. The overall power conversion efficiency is



improved from the light load to the heavy load. In this design, the power conversion efficiency can be maintained from 88.19 to 93.41%, when the load current is changed from 1.06 to 119 A. Compared with the traditional fixed multi-phase DC–DC buck regulator design, this flexible multi-phase design increases the power conversion efficiency by  $\sim 2\text{--}23\%$ .

In the future, research will be conducted about both the efficiency relationship of the output voltage and the load current adjustment, in order to achieve an even better degree of power conversion efficiency.

## 5 References

- Huang, T., Bai, Y., Kuan, H.: 'Improvement of the power conversion efficiency of a personal computer'. Int. Symp. on Industrial Electronics, 2013, pp. 1–6
- Singh, S., Bist, V., Singh, B., *et al.*: 'Power factor correction in switched mode power supply for computers using canonical switching cell converter', *IET Power Electron.*, 2015, **8**, (2), pp. 234–244
- Su, J., Lin, C.: 'Auto-tuning scheme for improved current sharing of multiphase DC–DC converters', *IET Power Electron.*, 2012, **5**, (9), pp. 1605–1613
- Grandi, G., Loncarski, J.: 'Analysis of dead-time effects in multi-phase voltage source inverters'. IET Int. Conf. on Power Electronics, 2012, pp. 1–6
- Govindaraju, C.: 'Efficient sequential switching hybrid modulation techniques for multiphase multilevel inverters', *IET Power Electron.*, 2011, **4**, (5), pp. 557–569
- Jinping, W., Jianping, X.: 'A novel PWM control method for switching dc–dc converters with improved dynamic response performance'. Int. Symp. on Power Electronics for Distributed Generation Systems, 2010, pp. 85–88
- Lin, B., Chien, C.: 'Analysis and implementation of a new soft switching DC/DC PWM converter', *IET Power Electron.*, 2013, **6**, (1), pp. 202–213
- Lin, B., Cheng, P.: 'Analysis of an interleaved zero-voltage switching/zero current switching resonant converter with duty cycle control', *IET Power Electron.*, 2013, **6**, (2), pp. 374–382
- Lin, B., Liu, C.: 'Implementation of a parallel zero-voltage switching DC–DC converter with fewer active switches', *IET Power Electron.*, 2012, **5**, (9), pp. 1651–1659
- Wang, C., Lin, C., Hsu, S., *et al.*: 'Analysis, design and performance of a zero-current switching pulse-width-modulation interleaved boost DC/DC converter', *IET Power Electron.*, 2014, **7**, (9), pp. 2437–2445
- Cheung, C., Qiu, W., Chen, E., *et al.*: 'Phase doubler for high power voltage regulators'. Int. Conf. on Applied Power Electronics Conf. and Exposition, 2010, pp. 1081–1086
- Tsai, C., Kuo, C., Tsai, M.: 'Design and implementation of a 16 phases DC/DC buck converter'. Int. Conf. on Electric Information and Control Engineering, 2011, pp. 1277–1280
- Bai, Y., Tsai, C.: 'Design and implementation of a low-power workstation'. Canadian Conf. on Electrical and Computer Engineering, 2009, pp. 880–885
- Bai, Y., Lin, C.: 'Using a hybrid LDO regulator and a switching regulator circuit to reduce the power consumption in the light load operation of a server motherboard'. Canadian Conf. on Electrical and Computer Engineering, 2015, pp. 547–552
- Lu, L., Wenxi, Y., Zhengyu, L.: 'Multi-mode control strategy in three-level DC–DC converter for higher efficiency operation under light-load and standby conditions'. Int. Conf. on Applied Power Electronics Conf. and Exposition, 2015, pp. 921–926
- Pan, H., He, C., Ajmal, F., *et al.*: 'Pulse-width modulation control strategy for high efficiency LLC resonant converter with light load applications', *IET Power Electron.*, 2014, **7**, (11), pp. 2887–2894
- Tu, S., Chiu, M.: 'Digital pulse-width modulation controller based on fully table look-up for system-on-a-chip applications', *IET Power Electron.*, 2013, **6**, (9), pp. 1778–1785
- Zumel, P., Fernandez, C., Castro, A., *et al.*: 'Efficiency improvement in multiphase converter by changing dynamically the number of phases'. Int. Conf. on Power Electronics Specialists, 2006, pp. 1–6
- Qiu, W., Cheung, C., Xiao, S., *et al.*: 'Power loss analyses for dynamic phase number control in multiphase voltage regulators'. Int. Conf. on Applied Power Electronics Conf. and Exposition, 2009, pp. 102–108
- Cheung, C., Qiu, W., Houston, J., *et al.*: 'Design considerations of auto phase number control in multiphase voltage regulators'. Int. Conf. on Applied Power Electronics Conf. and Exposition, 2012, pp. 1253–1257
- Luo, A., Jin, G., Xiao, H., *et al.*: 'Simple control method for three-phase pulse-width modulation rectifier of switching power supply under unbalanced and distorted supply voltages', *IET Power Electron.*, 2014, **7**, (10), pp. 2572–2581